Infrared Physics and Technology 93 (2018) 77–80

Contents lists available at ScienceDirect

Infrared Physics & Technology

journal homepage: www.elsevier.com/locate/infrared

Regular article

Sol-gel synthesis and enhanced 1.54 µm emission in Y_2O_3:Yb^{3+}, Er^{3+} nanophosphors co-doped with Ce^{3+} ions

Nengli Wang*, Jianfeng He, Kexin Ye, Xiaojiao Song, Taiwen Li

School of Materials Science and Engineering, Changchun University of Science and Technology, Changchun 130022, China

ARTICLE INFO

Keywords:
Sol-gel synthesis
Y_2O_3 nanoparticles
Enhanced 1.54 µm emission

ABSTRACT

Nano-sized Y_2O_3:Yb^{3+}, Er^{3+} phosphors were synthesized by sol-gel method and characterized by X-ray diffraction, scanning electron microscope, near-infrared and upconversion fluorescence spectroscopy. The phosphors calcined at 1100 °C for 2 h were confirmed to be cubic Y_2O_3 phase with well-crystallized particles. With the introduction of Ce^{3+} ions at proper doping concentration, the 1.534 µm emission of Er^{3+} was found to be greatly enhanced, while the green and red upconversion emission intensity obviously decreased. The enhancement of 1.534 µm emission could be attributed to the phonon-assisted energy transfer process between Ce^{3+} and Er^{3+} ions.

1. Introduction

The near-infrared (NIR) emission at around 1.54 µm, which corresponds to the $^4I_{13/2} \rightarrow {}^4I_{15/2}$ transition of Er^{3+} ions, has attracted particular attentions from researchers in recent years. The 1.54 µm emission band is eye-safe and has been found wide range of applications in fiber amplifiers, solar cells, eye-safe infrared laser, laser ranging and telecommunications, doppler wind lidar, *in vivo* imaging at NIR-II biological window, and so on [1–10]. Generally, in order to obtain 1.54 µm NIR emission, Er^{3+} ions are excited by 980 nm excitation source from ground state $^4I_{15/2}$ to the excited state $^4I_{11/2}$, and then non-radiatively relax to $^4I_{13/2}$ level, transition of $^4I_{13/2} \rightarrow {}^4I_{15/2}$ produces 1.54 µm emission. But in fact, a large part of electrons at $^4I_{11/2}$ do not relax to $^4I_{13/2}$, they may be excited to $^4F_{7/2}$ and then transit to ground state $^4I_{15/2}$ to produce green and red upconversion (UC) emission. So, Relation between UC and 1.54 µm emission is competitive, UC process is unfavorable to the obtainment of high-intensity 1.54 µm emission in Yb^{3+}/Er^{3+} co-doped luminescent materials. Researches revealed that in Er^{3+}-doped glasses and crystals, co-doping of Ce^{3+} can increase the non-radiative transition probability of $^4I_{11/2} \rightarrow {}^4I_{13/2}$ of Er^{3+}, so can enhance the fluorescence characteristics around 1.54 µm [11–13]. The enhancement of NIR emission located at 1540 nm was also observed in the CeO_2:Er^{3+}, Yb^{3+} inverse opals with the photonic band gaps at 500 and 450 nm when the wavelength of the excitation overlapped the photonic band edge, which was attributed to slow light effect of photonic crystals [14].

Yb^{3+} ion possesses two $4f^{13}$ manifolds $^2F_{5/2}$ and $^2F_{7/2}$ with energy gap of about 10,000 cm^{-1}, which matches well with the emission wavelength of many commercially available 980 nm laser diode (LD). The $^2F_{5/2} \rightarrow {}^2F_{7/2}$ transition of Yb^{3+} overlaps with the $^4I_{15/2} \rightarrow {}^4I_{11/2}$ transition of the Er^{3+} at around 940–1100 nm, so co-doping of Yb^{3+} with Er^{3+} can enhance the pumping efficiency and facilitate the application of 980 nm LD in compact optical amplifiers and integrated devices with Er^{3+}-doped materials. Cubic sesquioxide yttria (Y_2O_3) has attracted research focus as an optical host material due to its superior physical and chemical properties, such as high thermal conductivity, broad transparency range and relatively low phonon energy [15–17]. Therefore, Yb^{3+}/Er^{3+} co-doped Y_2O_3 (Y_2O_3:Yb^{3+}, Er^{3+}) materials have potentials as a promising 1.54 µm luminescence materials. Until now, there are few reports about the effects of UC emission on the 1.54 µm luminescence properties in Y_2O_3:Yb^{3+}, Er^{3+} system. In this work, Y_2O_3:Yb^{3+}, Er^{3+} nanophosphors were synthesized by sol–gel method, the effects of Ce^{3+} ion on the NIR and UC luminescence property of Y_2O_3:Yb^{3+}, Er^{3+} were investigated. With the introduction of Ce^{3+} ions, an enhanced 1.54 µm emission from the Y_2O_3:Yb^{3+}, Er^{3+} phosphors was observed. The mechanism of the enhancement of 1.54 µm emission was also discussed.

2. Experimental

Stoichiometric amounts of Y_2O_3, Yb_2O_3, Er_2O_3 and CeO_2 (all 99.99% in purity) were weighed according to the chemical formula $(Y_{0.928-x}Yb_{0.07}Er_{0.002}Ce_x)_2O_3$ (x = 0, 0.002, 0.004, 0.008, 0.012 and 0.016). The oxides were dissolved in nitric acid and diluted with

---

* Corresponding author.
E-mail address: wang_nengli@163.com (N. Wang).

https://doi.org/10.1016/j.infrared.2018.07.023
Received 6 May 2018; Received in revised form 16 July 2018; Accepted 17 July 2018

deionized water and mixed thoroughly on a magnetic stirrer for 2 h to obtain a metal nitrate solution. Glycine (NH_2CH_2COOH), which acted as a chelating agent with amount of $[RE^{3+}]/[glycine] = 1$ was added into the nitrate solution, the solution kept heating and stirring at 80 °C for 4 h to obtained wet gel, which was then dried at about 100 °C for 9 h to get dry gel. The dry gel was crushed in an agate mortar and then calcined at different temperatures for 2 h to obtain the samples.

X-ray diffraction (XRD) measurement was conducted on a Rigaku Ultima IV diffractometer with CuKα radiation source for phase identification. Morphology of the phosphor was characterized by a FEG scanning electron microscope (FE-SEM, Model XL30, FEI Company). The UC emission spectra were measured by a Shimadzu RF-5301PC spectrometer with an optical fiber-coupled 980 nm LD as the excitation source. The NIR excitation and emission spectra were measured using a Jobin Yvon Spex Fluorolog-3 spectrometer. All the characterizations were performed at room temperature.

3. Results and discussion

3.1. XRD pattern and morphology of the phosphors

Fig. 1(a) shows the XRD patterns of the synthesized $Y_2O_3:Yb^{3+}$, Er^{3+}, Ce^{3+} phosphors calcined at 1100 °C for 2 h. All diffraction peaks of the samples were in good accordance with pure cubic Y_2O_3 phase (JCPDS no. 41-1105), indicating a complete crystallization of the phosphors. The ionic radius of Ce^{3+} ion (1.034 Å) is larger than that of Y^{3+} ion (0.88 Å), the doping of Ce^{3+} into Y_2O_3 host led to an expansion of the unit cell and an increase of the interplanar spacing d. The increase of d can lead to a decrease of θ value according to the Bragg's law $2d\sin\theta = \lambda$ (where d, λ and θ represents interplanar spacing, X-ray wavelength, and bragg angle, respectively). Thus, with the increase of Ce^{3+} doping concentration, the XRD patterns slightly shifted to the left compared with the standard JCPDS pattern, which can be seen in Fig. 1(a). It can be seen from Fig. 1(b) that the phosphor particles showed spherical morphology and uniform particle size distribution. The average particle size was about 70 to 80 nm in diameter, which was in the nanoscale range.

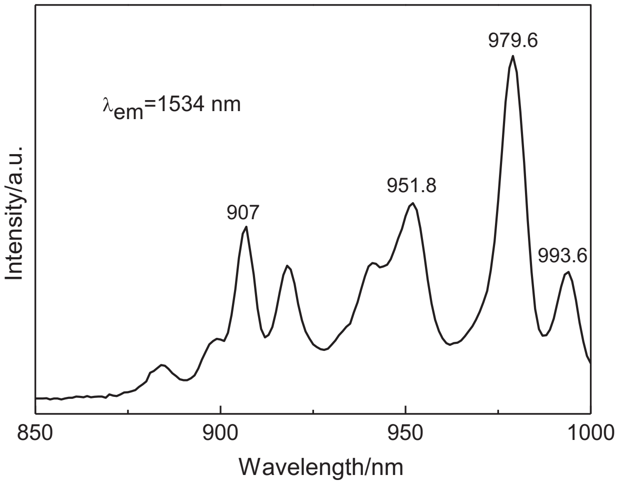

Fig. 2. NIR excitation spectrum of the $Y_2O_3:Yb^{3+}$, Er^{3+}, Ce^{3+} phosphors.

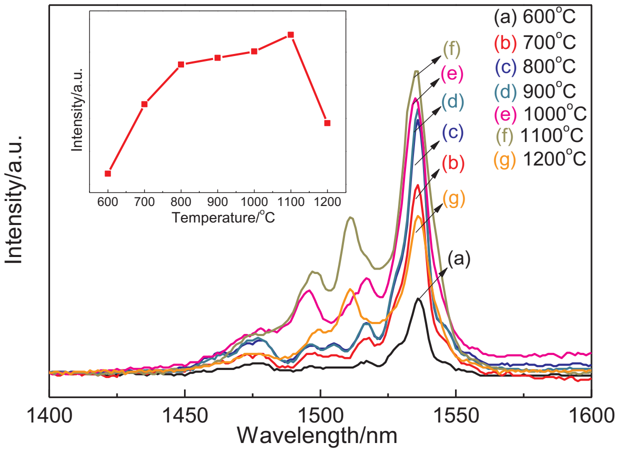

Fig. 3. NIR emission spectra of the $Y_2O_3:Yb^{3+}$, Er^{3+}, Ce^{3+} phosphors calcined at different temperatures.

3.2. NIR spectra of the phosphors

Fig. 2 shows the excitation spectrum of the phosphor with the monitoring wavelength of 1534 nm. The spectrum consisted of a series of peaks ranging from 900 to 1000 nm, the excitation bands was broad, and the 980 nm excitation wavelength had the highest 1534 nm emission intensity, which made it suitable to be coupled by the commercially available 980 nm LD. Fig. 3 shows the NIR emission spectra of $Y_2O_3:Yb^{3+}$, Er^{3+}, Ce^{3+} phosphors calcined at different temperatures (λ_{ex} = 980 nm). The main emission peak located at 1534 nm, which can be assigned to the $^4I_{13/2} \rightarrow {}^4I_{15/2}$ transition of Er^{3+} ion. With increase of calcination temperature, the 1534 nm emission intensity increased and reached the maximum when the temperature reached 1100 °C. But a continuous increase of calcination temperature did not further enhance the emission intensity, the emission intensity decreased when the calcination temperature reached 1200 °C, which can be seen

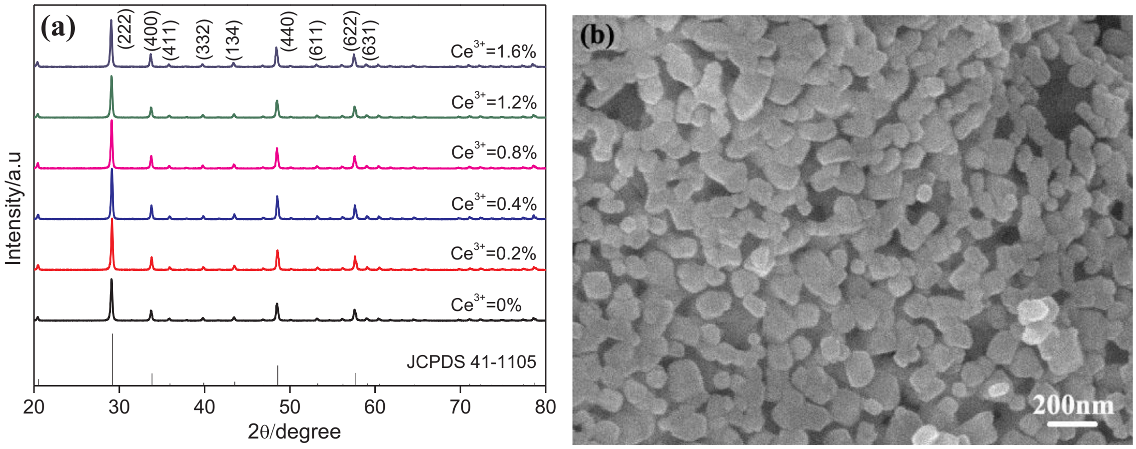

Fig. 1. XRD patterns of the phosphors with different Ce^{3+} doping concentrations (a) and SEM image of the phosphors (b).